

# A temporal shift in the circuits mediating retrieval of fear memory

Fabricio H. Do-Monte<sup>1,2</sup>, Kelvin Quiñones-Laracuente<sup>1,2</sup> & Gregory J. Quirk<sup>1,2</sup>

Fear memories allow animals to avoid danger, thereby increasing their chances of survival. Fear memories can be retrieved long after learning<sup>1,2</sup>, but little is known about how retrieval circuits change with time<sup>3,4</sup>. Here we show that the dorsal midline thalamus of rats is required for the retrieval of auditory conditioned fear at late (24 hours, 7 days, 28 days), but not early (0.5 hours, 6 hours) time points after learning. Consistent with this, the paraventricular nucleus of the thalamus (PVT), a subregion of the dorsal midline thalamus, showed increased *c-Fos* expression only at late time points, indicating that the PVT is gradually recruited for fear retrieval. Accordingly, the conditioned tone responses of PVT neurons increased with time after training. The prelimbic (PL) prefrontal cortex, which is necessary for fear retrieval<sup>5–7</sup>, sends dense projections to the PVT<sup>8</sup>. Retrieval at late time points activated PL neurons projecting to the PVT, and optogenetic silencing of these projections impaired retrieval at late, but not early, time points. In contrast, silencing of PL inputs to the basolateral amygdala impaired retrieval at early, but not late, time points, indicating a time-dependent shift in retrieval circuits. Retrieval at late time points also activated PVT neurons projecting to the central nucleus of the amygdala, and silencing these projections at late, but not early, time points induced a persistent attenuation of fear. Thus, the PVT may act as a crucial thalamic node recruited into cortico-amygdalar networks for retrieval and maintenance of long-term fear memories.

The association between a conditioned stimulus (for example, a tone) and an aversive event (an electrical shock) can be retrieved throughout the lifetime of an animal<sup>9–11</sup>. This tone–shock association is stored in the basolateral amygdala (BLA) and the central nucleus of the amygdala (CeA)<sup>12–15</sup>, but the circuits necessary for retrieval of this memory at various times after learning are not well understood. The BLA receives

inputs from the PL<sup>16,17</sup>, a region necessary for fear retrieval<sup>5–7</sup>. The PL also projects densely to the dorsal midline thalamus (dMT)<sup>8</sup>, which in turn projects to the CeA<sup>18</sup>. Thus, the dMT could coordinate fear responses with adaptive responses such as stress, sleep and foraging through its connections with the hypothalamus or nucleus accumbens<sup>8,19</sup>. We previously observed that the dMT is necessary for fear retrieval 24 h after conditioning, but not earlier<sup>20</sup>. Here, to test directly the hypothesis that retrieval circuits change with time, we used pharmacological, immunocytochemical, unit-recording and optogenetic techniques.

We found that inactivating the dMT with the GABA<sub>A</sub> (γ-aminobutyric acid type A) receptor agonist muscimol shortly after conditioning (0.5 or 6 h) had no effect on fear retrieval, but inactivating the dMT at later time points (24 h, 7 d and 28 d) impaired retrieval (Fig. 1a–c; conditioning levels shown in Extended Data Fig. 1a–e). The next day, in the absence of drug, retrieval remained impaired in the 7 d and 28 d groups (Fig. 1d), suggesting that dMT activity may be necessary for the maintenance of fear memory. In support of this, retrieval was still impaired 1 week after the initial retrieval test (day 14, see Extended Data Fig. 2a). Inactivation of the dMT without retrieval had no effect (Extended Data Fig. 2b), suggesting a possible role of the dMT in memory reconsolidation. Although intra-dMT infusion of drugs that block reconsolidation had no effect (Extended Data Fig. 2c, d), dMT activity could be facilitating memory reconsolidation in downstream structures (such as the amygdala). Thus, with the passage of time, dMT activity becomes increasingly necessary first for retrieval and later for maintenance of fear memories.

Next, we used the neural activity marker *c-Fos* to determine when the dMT is activated by conditioning. After training, exposure to conditioned tones induced robust freezing at 6 h, 24 h and 7 d time points (Extended Data Fig. 3a–c), but triggered different patterns of neuronal

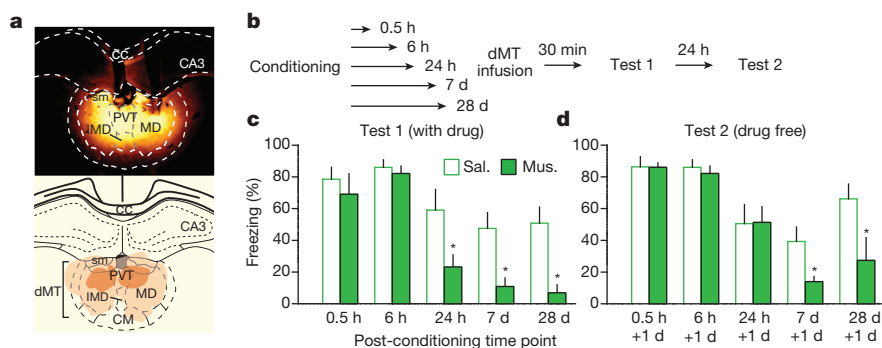


**Figure 1** | The dMT is necessary for retrieval of fear at late, but not early, time points after conditioning. **a**, Top, representative micrograph showing the site of fluorescent muscimol (Mus.) injection into dMT. Bottom, orange areas represent the minimum (dark) and the maximum (light) spread of muscimol into the dMT. cc, corpus callosum; IMD, intermediodorsal nucleus of the thalamus; MD, mediodorsal thalamus; sm, stria medullaris. **b**, Experimental design. **c**, Left, freezing to conditioned tones after infusion of saline (Sal., white) or muscimol (green) at different post-conditioning time

points. Muscimol impaired freezing ( $F_{(4,73)} = 3.31$ ,  $P = 0.01$ ) at 24 h ( $P = 0.002$ ,  $n = 8$  per group), 7 d ( $P = 0.002$ ,  $n = 14$  per group) and 28 d ( $P < 0.001$ ,  $n = 10$  for Sal.,  $n = 6$  for Mus.), but not at 0.5 h or 6 h ( $P > 0.99$ ,  $n = 6$  per group). Right, the next day, persistent attenuation of freezing ( $F_{(2,54)} = 4.78$ ,  $P = 0.011$ ) was observed at 7 d ( $P = 0.013$ ) and 28 d ( $P = 0.04$ ), but not at 24 h ( $P = 0.35$ ). Two-way ANOVA followed by Tukey's post-hoc test. Data are mean  $\pm$  s.e.m. in blocks of two trials; \* $P < 0.05$ .

<sup>1</sup>Department of Psychiatry, University of Puerto Rico School of Medicine, PO Box 365067, San Juan 00936, Puerto Rico. <sup>2</sup>Department of Anatomy & Neurobiology, University of Puerto Rico School of Medicine, P.O. Box 365067, San Juan 00936, Puerto Rico.

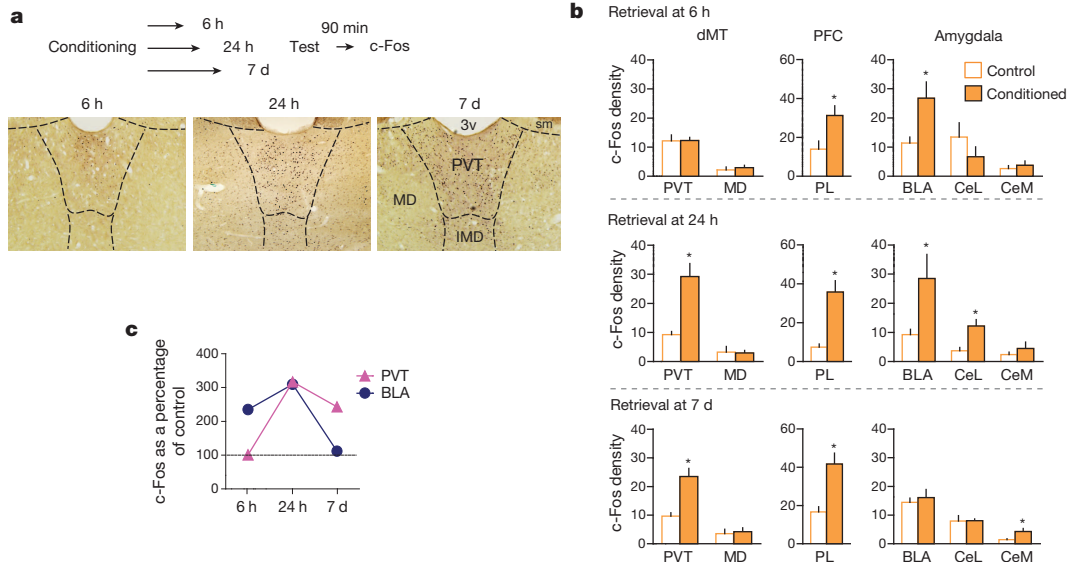


**Figure 2 | c-Fos expression induced by fear retrieval at different time points after conditioning.** **a**, Top, schematic for c-Fos experiments. Bottom, micrographs showing c-Fos expression in the dMT in the conditioned groups following fear retrieval at 6 h, 24 h and 7 d time points. **b**, Top, fear retrieval at 6 h ( $n = 4-5$  per group) increased the number of c-Fos-positive neurons (per  $0.1 \text{ mm}^2$ ) in the PL prefrontal cortex ( $P = 0.03$ ,  $t = 2.65$ ) and BLA ( $P = 0.02$ ,  $t = 2.85$ ), but not in the PVT ( $P = 0.96$ ,  $t = 0.04$ ). Middle, fear retrieval at 24 h ( $n = 3-4$  per group) increased the number of c-Fos positive neurons in the PL ( $P = 0.002$ ,  $t = -5.43$ ), PVT ( $P = 0.007$ ,  $t = 3.22$ ),

BLA ( $P = 0.04$ ,  $t = -2.67$ ) and the lateral portion of the central nucleus of the amygdala (CeL;  $P = 0.01$ ,  $t = -3.80$ ). Bottom, fear retrieval at 7 d ( $n = 5-6$  per group) increased the number of c-Fos-positive neurons in the PL ( $P = 0.002$ ,  $t = 4.21$ ), PVT ( $P < 0.001$ ,  $t = 4.83$ ) and the medial portion of the central nucleus of the amygdala (CeM;  $P = 0.02$ ,  $t = 2.69$ ). **c**, c-Fos levels (as a percentage of control) in the PVT and BLA after fear retrieval at 6 h, 24 h and 7 d time points. Data are mean  $\pm$  s.e.m.; unpaired  $t$ -test between control and conditioned groups;  $*P < 0.05$ .

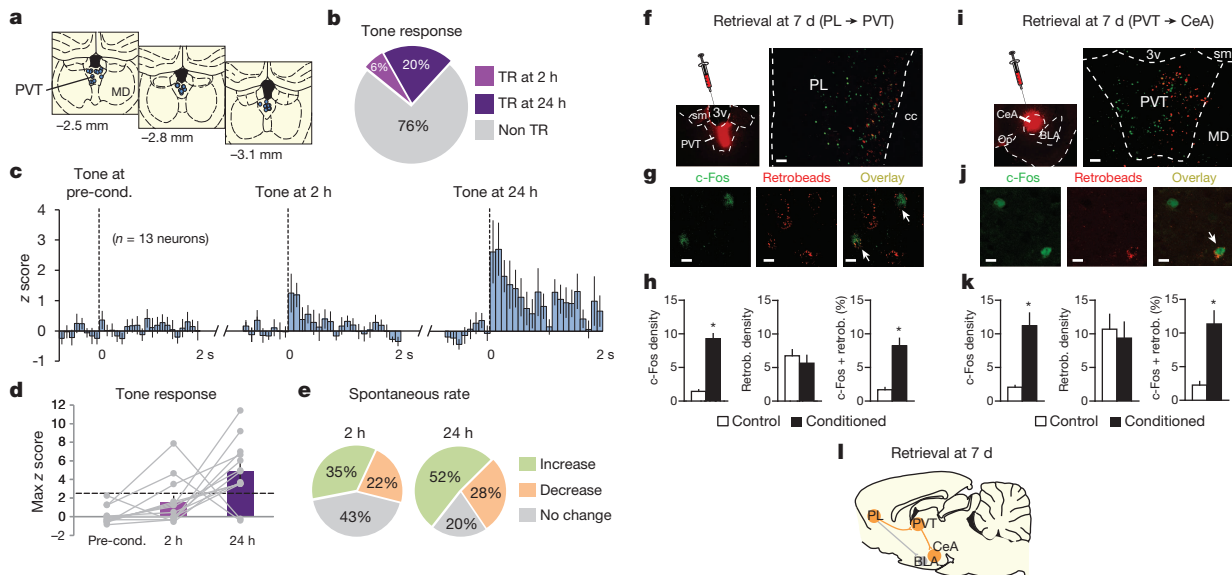


**Figure 3 | Time-dependent increases in tone responses of PVT neurons following fear conditioning.** **a**, Diagram of recording placements in the PVT. Coordinates from bregma. **b**, Percentage of tone-responsive (TR) neurons at 2 h and 24 h after conditioning ( $n = 54$  neurons, 6% tone responsive at 2 h, 20% tone responsive at 24 h, Fisher's exact test,  $P = 0.04$ ). **c**, Average peri-stimulus time histograms of all PVT neurons that were significantly tone responsive at either 2 h or 24 h after conditioning ( $n = 13$  neurons, 100 ms bins). **d**, Maximum z score for group data (bars) or individual data (grey lines,  $n = 13$  neurons). Dashed line indicates a z score criterion of 2.58. **e**, Changes in spontaneous firing rates of PVT neurons at 2 h (left) and 24 h (right) after conditioning, compared to pre-conditioning. Changes at 24 h were significantly greater than 2 h ( $n = 54$  neurons; 24 h = 80%; 2 h = 57%, Fisher's exact test,  $P = 0.02$ ). **f**, Left, micrograph showing site of retrobead infusion into the PVT. Right, micrograph showing PL neurons projecting to the PVT (retrogradely labelled, red) expressing immunoreactivity for c-Fos (green) after fear retrieval at 7 d. 3v, third ventricle. Scale bar, 100  $\mu\text{m}$ . **g**, Confocal images showing c-Fos labelling (left), retrobead labelling (middle), and overlay (right) of PVT-projecting PL neurons (white arrows). Scale bar,

10  $\mu\text{m}$ . **h**, Fear retrieval at 7 d increased the number of c-Fos-positive neurons (per  $0.1 \text{ mm}^2$ ) in the PL (left,  $P = 0.003$ ,  $t = 8.74$ ), but the number of retrogradely labelled PL neurons was the same between groups (middle,  $P = 0.51$ ,  $t = -0.7$ ). Retrieval increased the percentage of retrogradely labelled PL neurons expressing c-Fos (right,  $P = 0.004$ ,  $t = 4.83$ ;  $n = 3-4$  per group). **i**, Left, micrograph showing the site of retrobead infusion into the CeA. Right, micrograph showing PVT neurons projecting to the CeA (retrogradely labelled, red) expressing immunoreactivity for c-Fos (green) after fear retrieval at 7 d. Scale bar, 100  $\mu\text{m}$ . **j**, Confocal images showing c-Fos labelling (left), retrobead labelling (middle), and overlay (right) of CeA-projecting PVT neurons (white arrow). Scale bar, 10  $\mu\text{m}$ . **k**, Fear retrieval at 7 d increased the number of c-Fos-positive neurons (per  $0.1 \text{ mm}^2$ ) in the PVT (left,  $P = 0.03$ ,  $t = 3.71$ ), but the number of retrogradely labelled PVT neurons was the same between groups (middle,  $P = 0.79$ ,  $t = -0.28$ ). Retrieval increased the percentage of retrogradely labelled PVT neurons expressing c-Fos (right,  $P = 0.03$ ,  $t = 3.61$ ;  $n = 2-3$  per group). **l**, Schematic of the potential circuit mediating fear retrieval at the 7 d time point. Data are mean  $\pm$  s.e.m.; unpaired  $t$ -test between control and conditioned groups;  $*P < 0.05$ .

activation (Fig. 2a, b). The mediodorsal subdivision of the dMT showed no conditioned activation at any time point, whereas the PL showed activation at all three time points. This suggests that the PL is necessary for retrieval at both early and late time points, which we confirmed with muscimol (Extended Data Fig. 3d–f). Retrieval at 6 h activated PL and BLA, but not PVT, neurons, whereas retrieval at 7 d activated PL and PVT, but not BLA, neurons. Retrieval at 7 d also activated the medial portion of the central amygdala (CeM), suggesting that retrieval at 7 d may involve PL–PVT and PVT–CeA pathways. But at 24 h, both targets of the PL (BLA and PVT) were activated (Fig. 2b, c), consistent with a gradual shift in retrieval circuits from the PL–BLA to the PL–PVT.

Our c-Fos activation pattern that we observed (Fig. 2b) suggests that activation of PVT neurons at 7 d may involve inputs from the PL and outputs to the CeA. To address this further, we injected a retrograde tracer (retrobeads) into either the PVT or CeA and measured co-labelling with c-Fos in the PL and PVT, respectively. Accordingly, retrieval at 7 d activated PL neurons projecting to the PVT (Fig. 3f–h), plus PVT neurons projecting to the CeA (Fig. 3i–k). Taken together, our data suggest that PL–PVT and PVT–CeA pathways may be necessary for fear retrieval at late (7 d), but not early (6 h), time points (Fig. 3l).

conditioning (24 h = 11 of 54, 20%; 2 h = 3 of 54, 6%; Fisher's exact test,  $P = 0.04$ ; Fig. 3a–c). Moreover, the average magnitude of tone responses increased significantly from 2 h to 24 h in the same set of neurons ( $F_{(2,36)} = 13.29$ ,  $P = 0.003$ , Fig. 3c). Notably, 12 out of 13 PVT neurons that were tone responsive at 24 h were not tone responsive at 2 h (Fig. 3d), consistent with a time-dependent recruitment of PVT neurons. In addition to tone responses, conditioning-induced changes in the spontaneous firing rate of PVT neurons were greater at 24 h compared to 2 h (24 h = 43 of 54, 80%; 2 h = 31 of 54, 43%; Fisher's exact test,  $P = 0.02$ ; Fig. 3e).

The c-Fos activation pattern that we observed (Fig. 2b) suggests that activation of PVT neurons at 7 d may involve inputs from the PL and outputs to the CeA. To address this further, we injected a retrograde tracer (retrobeads) into either the PVT or CeA and measured co-labelling with c-Fos in the PL and PVT, respectively. Accordingly, retrieval at 7 d activated PL neurons projecting to the PVT (Fig. 3f–h), plus PVT neurons projecting to the CeA (Fig. 3i–k). Taken together, our data suggest that PL–PVT and PVT–CeA pathways may be necessary for fear retrieval at late (7 d), but not early (6 h), time points (Fig. 3l).

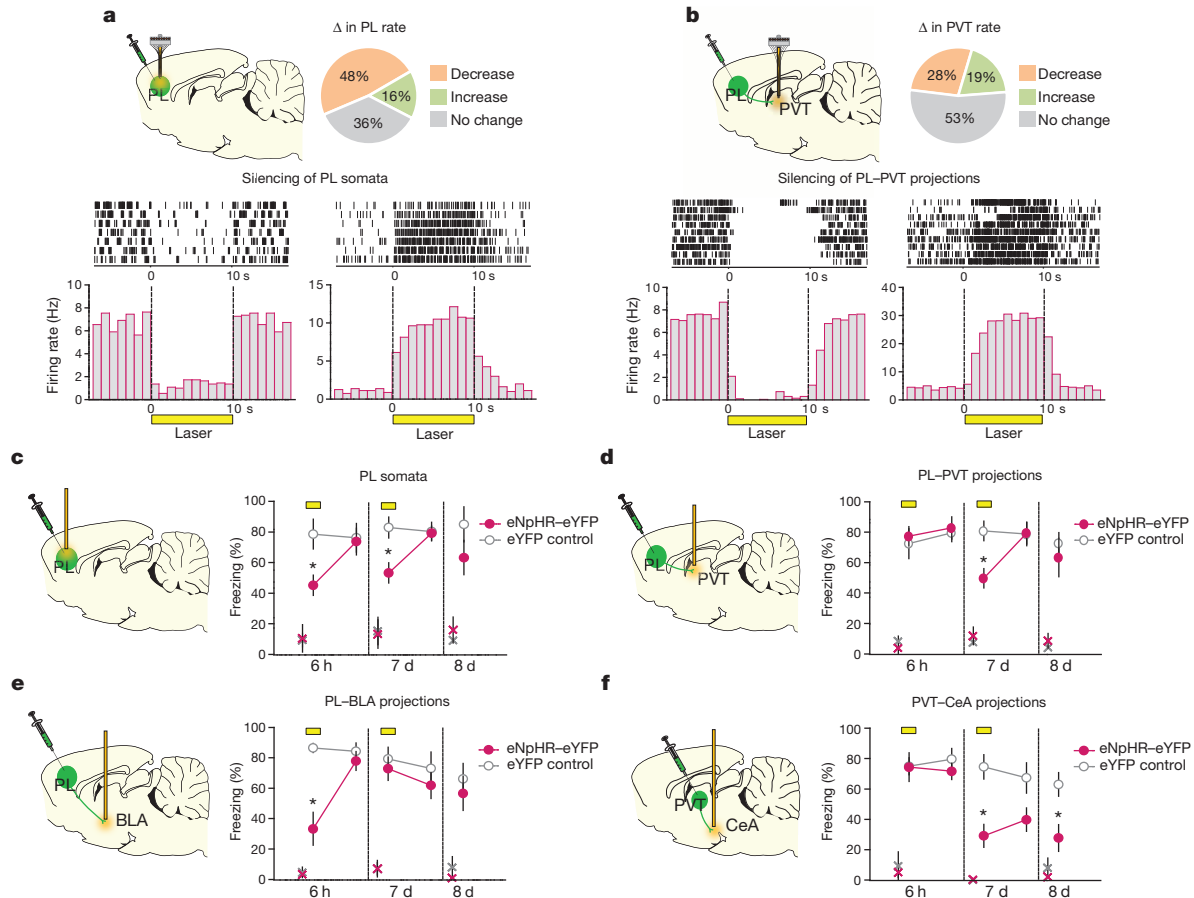


**Figure 4 | Time-dependent shift of retrieval circuits after conditioning.**

**a**, Top, changes in PL firing rate with illumination of PL in rats expressing eNpHR–eYFP in PL ( $n = 50$  neurons; 48% decreased, 16% increased; 36% did not change; unpaired  $t$ -test;  $P < 0.05$ ). Bottom, raster plot and peri-stimulus time histogram of representative PL neurons responding to illumination in rats expressing eNpHR–eYFP in PL. PL neurons showed inhibition (left) or excitation (right). **b**, Top, changes in PVT firing rate after illumination of PL terminals in the PVT in rats expressing eNpHR–eYFP in the PL ( $n = 47$  neurons; 28% decreased, 19% increased; 53% did not change; unpaired  $t$ -test;  $P < 0.05$ ). Bottom, raster plot and peri-stimulus time histogram of representative PVT neurons responding to illumination of PL inputs in the PVT in rats infused with eNpHR–eYFP in the PL. PVT units showed inhibition (left) or excitation (right). **c**, Illumination (yellow bar) of PL somata reduced

freezing to tones at both 6 h ( $F_{(1,10)} = 15.1$ ,  $P = 0.003$ ) and 7 d ( $F_{(1,10)} = 20.3$ ,  $P = 0.002$ ) in the eNpHR–eYFP group ( $n = 7$ ), compared to the eYFP control group ( $n = 5$ ). **d**, Illumination of PL inputs in the PVT significantly reduced freezing at 7 d ( $F_{(1,9)} = 18.7$ ,  $P = 0.002$ ), but not 6 h ( $F_{(1,10)} = 0.06$ ,  $P = 0.81$ ) (eNpHR–eYFP,  $n = 7$ ; control,  $n = 4$ ). **e**, Illumination of PL inputs in the BLA significantly reduced freezing at 6 h ( $F_{(1,16)} = 26.0$ ,  $P < 0.001$ ), but not 7 d ( $F_{(1,16)} = 0.64$ ,  $P = 0.43$ ) (eNpHR–eYFP,  $n = 8$ ; control,  $n = 10$ ). **f**, Illumination of PVT inputs in the CeA significantly reduced freezing at 7 d ( $F_{(1,11)} = 11.9$ ,  $P = 0.005$ ), but not 6 h ( $F_{(1,11)} = 0.19$ ,  $P = 0.67$ ) (eNpHR–eYFP,  $n = 8$ ; control,  $n = 5$ ). Freezing remained reduced the day after illumination of CeA inputs to the PVT ( $P = 0.018$ ). Repeated-measures ANOVA followed by Tukey's post-hoc test. Data are mean  $\pm$  s.e.m. in blocks of 2 trials; \* $P < 0.05$ . 'x' denotes baseline (pre-tone) freezing levels.



To test these hypotheses directly, we used an optogenetic approach to silence specific projections at these two time points, within the same animal. The PL was infused with an adeno-associated viral vector (AAV-5) expressing the light-sensitive chloride pump halorhodopsin<sup>21</sup> combined with enhanced yellow fluorescent protein (eYFP), under the control of a CaMKII $\alpha$  promoter, favouring expression within pyramidal neurons (AAV5:CaMKII $\alpha$ ::eNpHR3.0-eYFP)<sup>22,23</sup>. In anaesthetized rats, laser illumination of PL somata reduced (24 out of 50 tested, 48%) or in some cases increased (8 out of 50 tested, 16%) the firing rate of PL neurons (Fig. 4a and Extended Data Fig. 5a–c). Neurons that reduced their rate showed shorter response latencies than neurons that increased their rate, suggesting direct versus indirect responses, respectively. Furthermore, silencing PL terminals within the PVT either reduced (13 out of 47 tested, 28%) or increased (9 out of 47 tested, 19%) the firing rates of PVT neurons (Fig. 4b and Extended Data Fig. 5d–f), without significant differences in response latency. Our observation of both short and long response latencies in PVT neurons (Extended Data Fig. 5f) suggests that the PL may influence the PVT both directly and indirectly.

We then determined the effects of PL silencing on retrieval of fear memory. Silencing PL somata impaired retrieval at both 6 h and 7 d (Fig. 4c and Extended Data Figs 1f, 6a and 10a); however, silencing PL projections to the PVT impaired retrieval at 7 d, but not at 6 h (Fig. 4d and Extended Data Figs 1g, 6b and 10b). In contrast, silencing PL projections to the BLA impaired retrieval at 6 h, but not at 7 d (Fig. 4e and Extended Data Figs 1h, 6c and 10c). Thus, fear retrieval initially depends on PL–BLA circuits, but shifts to PL–PVT circuits with the passage of time. This shift probably involves different ensembles of neurons, as PL neurons projecting to the PVT versus the BLA are located in different layers of the PL<sup>8,16</sup> (Extended Data Fig. 7).

We next questioned which outputs of the PVT could mediate fear retrieval. The PVT sends dense projections to the CeA<sup>18,19,24</sup>, and we observed that retrieval at 7 d activated PVT neurons projecting to the CeA (Fig. 3h). Accordingly, silencing PVT projections to the CeA impaired retrieval at 7 d, but not at 6 h (Fig. 4f and Extended Data Figs 1i, 6d and 10d). Retrieval remained impaired the day after silencing (day 8), suggesting that activation of PVT–CeA circuits is necessary for the maintenance of fear memory. It is unlikely that impaired retrieval at 7 d is caused by diffusion of the laser light from the CeA to the adjacent BLA because silencing BLA somata at 7 d did not impair retrieval (Extended Data Fig. 1j, 8, 10e). Silencing PVT–CeA projections during the inter-tone interval also had no effect (Extended Data Fig. 1k, 9), suggesting that the tone responses of PVT neurons (Fig. 3c) are essential for memory retrieval and maintenance. The necessity of PVT–CeA projections at late time points agrees with an accompanying study<sup>25</sup> showing that PVT inputs to the CeA are necessary for the long-term (24 h), but not short-term (3 h), induction of conditioning-induced plasticity in the CeA that encodes fear memory<sup>14</sup>.

Our findings suggest a time-dependent reorganization of the neural circuits required for fear memory retrieval. While fear behaviour appears constant with time, the circuits mediating this behaviour are not. Retrieval of fear memories long after conditioning may activate PL inputs to the PVT, which could excite PVT neurons projecting to the CeA, thereby activating CeA neurons to elicit fear responses. Recruitment of the PVT may serve to integrate fear with other adaptive responses such as stress<sup>26</sup>, thereby strengthening fear memory in amygdala circuits. Dysregulation of time-dependent changes in retrieval circuits may contribute to exacerbated fear responses occurring long after the traumatic event, for instance in individuals with anxiety disorders.

**Online Content** Methods, along with any additional Extended Data display items and Source Data, are available in the online version of the paper; references unique to these sections appear only in the online paper.

Received 10 February; accepted 3 November 2014.

Published online 19 January 2015.

1. Jasnow, A. M., Cullen, P. K. & Riccio, D. C. Remembering another aspect of forgetting. *Front. Psychol.* **3**, 175 (2012).

2. Wiltgen, B. J. & Tanaka, K. Z. Systems consolidation and the content of memory. *Neurobiol. Learn. Mem.* **106**, 365–371 (2013).
3. Sacco, T. & Sacchetti, B. Role of secondary sensory cortices in emotional memory storage and retrieval in rats. *Science* **329**, 649–656 (2010).
4. Restivo, L., Vetere, G., Bontempi, B. & Ammassari-Teule, M. The formation of recent and remote memory is associated with time-dependent formation of dendritic spines in the hippocampus and anterior cingulate cortex. *J. Neurosci.* **29**, 8206–8214 (2009).
5. Sierra-Mercado, D., Padilla-Coreano, N. & Quirk, G. J. Dissociable roles of prelimbic and infralimbic cortices, ventral hippocampus, and basolateral amygdala in the expression and extinction of conditioned fear. *Neuropsychopharmacology* **36**, 529–538 (2011).
6. Burgos-Robles, A., Vidal-Gonzalez, I. & Quirk, G. J. Sustained conditioned responses in prelimbic prefrontal neurons are correlated with fear expression and extinction failure. *J. Neurosci.* **29**, 8474–8482 (2009).
7. Courtin, J. et al. Prefrontal parvalbumin interneurons shape neuronal activity to drive fear expression. *Nature* **505**, 92–96 (2014).
8. Li, S. & Kirouac, G. J. Sources of inputs to the anterior and posterior aspects of the paraventricular nucleus of the thalamus. *Brain Struct. Funct.* **217**, 257–273 (2012).
9. LeDoux, J. E. Emotion circuits in the brain. *Annu. Rev. Neurosci.* **23**, 155–184 (2000).
10. Maren, S. Neurobiology of Pavlovian fear conditioning. *Annu. Rev. Neurosci.* **24**, 897–931 (2001).
11. Gale, G. D. et al. Role of the basolateral amygdala in the storage of fear memories across the adult lifetime of rats. *J. Neurosci.* **24**, 3810–3815 (2004).
12. Johansen, J. P., Cain, C. K., Ostroff, L. E. & LeDoux, J. E. Molecular mechanisms of fear learning and memory. *Cell* **147**, 509–524 (2011).
13. Rogan, M. T., Staubli, U. V. & LeDoux, J. E. Fear conditioning induces associative long-term potentiation in the amygdala. *Nature* **390**, 604–607 (1997).
14. Li, H. et al. Experience-dependent modification of a central amygdala fear circuit. *Nature Neurosci.* **16**, 332–339 10.1038/nn.3322 (2013).
15. Ciochi, S. et al. Encoding of conditioned fear in central amygdala inhibitory circuits. *Nature* **468**, 277–282 (2010).
16. Vertes, R. P. Differential projections of the infralimbic and prelimbic cortex in the rat. *Synapse* **51**, 32–58 (2004).
17. McDonald, A. J., Mascagni, F. & Guo, L. Projections of the medial and lateral prefrontal cortices to the amygdala: a *Phaseolus vulgaris* leucoagglutinin study in the rat. *Neuroscience* **71**, 55–75 (1996).
18. Vertes, R. P. & Hoover, W. B. Projections of the paraventricular and paratenial nuclei of the dorsal midline thalamus in the rat. *J. Comp. Neurol.* **508**, 212–237 (2008).
19. Moga, M. M., Weis, R. P. & Moore, R. Y. Efferent projections of the paraventricular thalamic nucleus in the rat. *J. Comp. Neurol.* **359**, 221–238 (1995).
20. Padilla-Coreano, N., Do-Monte, F. H. & Quirk, G. J. A time-dependent role of midline thalamic nuclei in the retrieval of fear memory. *Neuropharmacology* **62**, 457–463 (2012).
21. Gradinaru, V. et al. Molecular and cellular approaches for diversifying and extending optogenetics. *Cell* **141**, 154–165 (2010).
22. Liu, X. B. & Jones, E. G. Localization of alpha type II calcium calmodulin-dependent protein kinase at glutamatergic but not gamma-aminobutyric acid (GABAergic) synapses in thalamus and cerebral cortex. *Proc. Natl Acad. Sci. USA* **93**, 7332–7336 (1996).
23. Van den Oever, M. C. et al. Ventromedial prefrontal cortex pyramidal cells have a temporal dynamic role in recall and extinction of cocaine-associated memory. *J. Neurosci.* **33**, 18225–18233 (2013).
24. Li, S. & Kirouac, G. J. Projections from the paraventricular nucleus of the thalamus to the forebrain, with special emphasis on the extended amygdala. *J. Comp. Neurol.* **506**, 263–287 (2008).
25. Penzo, M. A. et al. The paraventricular thalamus controls a central amygdala fear circuit. *Nature* <http://dx.doi.org/10.1038/nature13978> (this issue).
26. Heyndael, W. et al. Orexins/hypocretins act in the posterior paraventricular thalamic nucleus during repeated stress to regulate facilitation to novel stress. *Endocrinology* **152**, 4738–4752 (2011).

**Acknowledgements** We thank G. Manzano-Nieves for help with the optogenetic experiments, A. C. Felix-Ortiz for technical advice, and K. M. Tye for comments on the manuscript. We thank K. Deisseroth for viral constructs and the UNC Vector Core Facility for viral packaging. This study was supported by the NIH grants R01-MH058883, and P50-MH086400, and a grant from the University of Puerto Rico President's Office to G.J.Q.; the MBR5-RISE Program (R25-GM061838) to K.Q.L.; and NSF grant DBI-0115825 and RCMI grant 8G12-MD007600 for the Confocal Microscope Facility.

**Author Contributions** F.H.D.-M. performed behavioural, immunocytochemical and optogenetic experiments. F.H.D.-M. and K.Q.-L. performed single-unit recording in anaesthetized rats. K.Q.-L. performed single-unit recording experiments in behaving rats. F.H.D.-M., K.Q.-L. and G.J.Q. designed the study, interpreted results, and wrote the paper.

**Author Information** Reprints and permissions information is available at [www.nature.com/reprints](http://www.nature.com/reprints). The authors declare no competing financial interests. Readers are welcome to comment on the online version of the paper. Correspondence and requests for materials should be addressed to F.H.D.-M. ([fabriciodomonte@gmail.com](mailto:fabriciodomonte@gmail.com)).

## METHODS

All procedures were approved by the Institutional Animal Care and Use Committee of the University of Puerto Rico School of Medicine in compliance with National Institutes of Health guidelines for the care and use of laboratory animals.

**Subjects.** A total of 266 male Sprague Dawley rats (Harlan Laboratories) weighing 300–360 g were housed and handled as described previously<sup>27</sup>. Rats were maintained on a restricted diet (18 g per day of standard rat chow) until they reached 85% of their original body weight. They were then trained to press a bar for food on a variable interval schedule of reinforcement (VI-60 s)<sup>27</sup>, except for unit recording experiments and Extended Data Fig. 2a. Pressing a bar for food ensures a constant level of activity in which freezing behaviour can be reliably measured during fear conditioning sessions<sup>27</sup>. For optogenetic experiments, rats were randomly assigned to each of the experimental groups. For muscimol inactivation and immunocytochemistry experiments, groups were assigned after matching for freezing levels during the conditioning session. Sample size was based on estimations by power analysis with a level of significance of 0.05 and a power of 0.9.

**Surgeries.** Rats were anaesthetized with isoflurane (5%) in an induction chamber. Rats were positioned in a stereotaxic frame (Kopf Instruments) and anaesthetized with isoflurane (2.5%) through a facemask. For muscimol inactivation experiments, double 26-gauge guide cannulas with 9 mm of length (Plastics One) were implanted targeting the dorsal midline thalamus (dMT; anteroposterior (AP), -2.6 mm from bregma; mediolateral (ML), ±0.6 mm from midline; dorsoventral (DV), -4.5 mm from skull surface) or the prelimbic cortex (PL; AP, +2.8 mm; ML, ±0.6 mm; DV, -2.6 mm)<sup>28</sup>. Stainless-steel obturators (33-gauge) were inserted into the guide cannulas to avoid obstructions until infusions were made. The cannula was fixed to the skull with anchoring screws and acrylic cement. For retrograde labelling experiments, a 0.5 µl syringe (Hamilton) was used to infuse 0.1 µl of green or red fluorescently labelled latex retrobeads (Lumafuor Inc.) per site. Retrobeads were chosen because they show very limited diffusion from the injection site even weeks after infusion.

For optogenetic experiments, a double 22-gauge guide cannula (9 mm length) was implanted targeting the PL. A single guide cannula (12 mm length) was implanted aiming at the paraventricular nucleus of the thalamus (PVT; AP, -2.6 mm; ML, ±2.0 mm; DV, -4.7 mm, 20° angle), or bilaterally implanted aiming at the basolateral amygdala (BLA; AP, -2.6 mm; ML, ±4.8 mm; DV, -7.6 mm) or the central amygdala (CeA; AP, -2.6 mm; ML, ±4.2 mm; DV, -6.7 mm). An injector extending 1 mm past the cannula tip was used to inject 0.5 µl of virus at a rate of 0.05 µl per min. After infusion, the injector was kept inside the cannula for 10 min to reduce back-flow. The injector was then removed and an optical fibre with 0.5 mm of projection was inserted into the cannula. Adhesive cement (C&B metabond; Parkell) was applied first, followed by acrylic cement to fix the guide cannula and the optical fibre to the skull. For unit-recording experiments, a moveable array of 16 microwires (50 µm, 2 × 8; NB Labs) was used to record from the PVT. After surgery, a triple antibiotic was applied and an analgesic (ketofen, 2 mg kg<sup>-1</sup>) was injected intramuscularly. All rats were allowed 5–7 days for recovery, except those used for optogenetic experiments, which were allowed 6–8 weeks for virus expression.

**Histology.** Upon completion of experiments, rats were transcardially perfused with 0.9% saline followed by 10% buffered formalin. Brains were extracted and stored in a 30% sucrose/10% formalin solution. Coronal frozen sections were cut 40 µm thick, mounted on slides, and observed in a microscope equipped with a fluorescent lamp (X-Cite, Series 120Q) and a digital camera. The spread of fluorescent muscimol or retrobeads, the presence of eYFP labelling, and the placement of the optical fibre tips were determined for each rat, and those located outside the target area were excluded from the statistical analysis.

**Drug infusion.** The GABA<sub>A</sub> agonist muscimol (fluorescent muscimol, BODIPY TMR-X conjugate, Sigma-Aldrich) was used to enhance GABA<sub>A</sub> receptor activity, thereby inactivating target structures. Infusions were made 30 min before testing at a rate of 0.2 µl per min (0.11 nmol per 0.2 µl per side), according to a previous study<sup>5</sup>. To inhibit the signal-regulated kinase/mitogen-activated protein kinase (ERK/MAPK) signalling cascade within dMT, U0126 (Tocris) was dissolved in 5% dimethylsulfoxide (DMSO) and 5% Tween 80, diluted to a concentration of 2 µg µl<sup>-1</sup>, and infused into the dMT (0.5 µl per side) at a rate of 0.25 µl per min immediately after retrieval test, according to a previous study<sup>29</sup>. To block the synthesis of proteins within the dMT, anisomycin (Sigma-Aldrich) was diluted in PBS and dissolved in 1 M HCl. The pH was adjusted back to 7.3 with NaOH and PBS until the solution reached a concentration of 125 µg µl<sup>-1</sup>. Anisomycin was infused into the dMT (0.5 µl per side) at a rate of 0.25 µl per min immediately after the retrieval test, according to a previous study<sup>30</sup>. Following infusion, the injectors were left in place for 1 min to allow the drug to diffuse.

**Auditory fear conditioning.** Rats were conditioned and tested in standard operant chambers (Coulbourn Instruments) located in sound-attenuating cubicles (Med Associates). The floor of the chambers consisted of stainless steel bars that delivered

a scrambled electric footshock. Between experiments, shock grids and floor trays were cleaned with soap and water, and chamber walls were cleaned with wet paper towels. Rats were conditioned with a pure tone (30 s, 4 KHz, 75 dB) paired with a shock delivered to the floor grids (0.5 s, 0.54 mA). All trials were separated by a variable interval averaging 3 min. Fear conditioning consisted of 5 habituation tones followed immediately by 7 conditioning tones that co-terminated with footshocks. To evaluate the role of dMT on fear retrieval, dMT was inactivated at 1 of 5 post-conditioning time points: 0.5 h, 6 h, 24 h, 7 d or 28 d, and rats were tested 30 min later in the same box with two tones. Only two post-conditioning time points were used for PL inactivation: 6 h or 7 d. A drug-free test was performed the day after infusion to test for fear maintenance. For immunocytochemistry experiments, naive rats (without bar-press training) were fear conditioned (conditioned group) or exposed to tones only (unconditioned group). Both groups received two test tones at either 6 h or 7 d after conditioning, and were perfused 90 min later. For all optogenetics experiments, rats were fear conditioned and tested with four tones at both 6 h and 7 d after conditioning. Laser illumination was delivered during the first two tones at each time point. The following day (day 8), two tones were delivered in the absence of illumination to test for fear memory maintenance. For unit-recording experiments, rats were fear conditioned and tested with four tones at 2 h and 24 h post-conditioning time points.

**Open field testing and bar-pressing for food.** Three days after completion of optogenetics experiments, rats were returned to the operant chambers to assess the effects of laser illumination on the motivation to press for food. The average press rate was compared between 5 min trials (laser off versus laser on), following a 5 min acclimation period. Rats pressing <3 or >30 presses per min during the acclimation period were eliminated (*n* = 3). Locomotor activity in the open field arena (90 cm diameter) was automatically assessed (ANY-Maze) by comparing the total distance travelled between 3 min trials (laser off versus laser on), following a 3 min acclimation period. The percentage of time spent in the centre of the open field (30 cm diameter) was used as an anxiety measurement.

**c-Fos immunocytochemistry.** Rats were deeply anaesthetized with sodium pentobarbital (450 mg kg<sup>-1</sup> intraperitoneal (i.p.)) and perfused transcardially with 100 ml of saline (0.9%), followed by 500 ml of 4% paraformaldehyde in 0.1 M phosphate buffer (pH 7.4). Brains were transferred to a solution of 30% sucrose in 0.1 M phosphate buffer at 4 °C for 48 h. Brains were then frozen and cut (40 µm) in the frontal plane of the medial prefrontal cortex, dorsal midline thalamus, and amygdala. A complete series of sections was processed for immunocytochemistry with anti-c-Fos serum raised in rabbit (Ab-5, Oncogene Science) at a dilution of 1:20,000 overnight. The primary antiserum was localized using a variation of the avidin–biotin complex system. Sections were incubated for 2 h at room temperature in a solution of biotinylated goat anti-rabbit IgG (1:200; Vector Laboratories) and placed in the mixed avidin–biotin horseradish peroxidase complex solution (1:200; ABC Elite kit, Vector Laboratories) for 90 min. Black immunoreactive nuclei labelled for c-Fos were visualized after 10 min of exposure to a chromogen solution containing 0.02% 3,3'-diaminobenzidine tetrahydrochloride with 0.3% nickel-ammonium sulfate (DAB-Ni) in 0.05 M Tris buffer (pH 7.6) followed by incubation for 5 min in a chromogen solution with glucose oxidase (10%) and D-glucose (10%). The reaction was stopped using potassium PBS (pH 7.4). Sections were mounted on gelatin-coated slides, dehydrated and cover slipped. Counter sections were stained for Nissl bodies, cover slipped and examined in an optical microscope to determine the anatomical boundaries of each structure. For fluorescent c-Fos labelling, sections were processed with the same antibody mentioned above at a dilution of 1:2,000 overnight, and placed in a fluorescent secondary-antibody Alexa Fluor 488 (1:200; Life Technologies) for 2 h. Sections were cover slipped with anti-fading mounting media (Vector Laboratories) and examined with both an epifluorescent and a confocal microscope.

**Immunoreactivity quantification.** c-Fos-positive cells were counted at 20× magnification of a brightfield microscope (Olympus, Model BX51) equipped with a digital camera. Images were generated for the prelimbic (PL) subregion of the medial prefrontal cortex (mPFC), the paraventricular (PVT) and the mediadorsal (MD) nucleus of the dorsal midline thalamus (dMT), the basolateral nucleus of the amygdala (BLA), the lateral portion of the central nucleus of the amygdala (CeL), and the medial portion of the central nucleus of the amygdala (CeM). Cells were considered positive for c-Fos-like immunoreactivity if the nucleus was the appropriate size (area ranging from 100 to 500 µm<sup>2</sup>) and shape (at least 50% of circularity), and was distinct from the background. c-Fos-positive cells were automatically counted (MetaMorph software version 6.1) and averaged for each hemisphere at distinct rostro-caudal levels. For the PL, counted sections at antero-posterior levels were +2.7 mm, +3.2 mm and +3.7 mm from the bregma. For dMT, counted sections at antero-posterior levels were -1.8 mm, -2.1 mm, -2.5 mm, -2.9 mm, -3.3 mm from the bregma. For amygdala, counted sections at antero-posterior levels were -2.3 mm and -2.8 mm from the bregma. The density of c-Fos positive cells (cells per 0.1 mm<sup>2</sup>) was calculated by dividing the number of c-Fos positive cells by the total area of each region. For fluorescent c-Fos and retrobeads quantification, images

were generated by using both an epifluorescent microscope (X-Cite, Series 120Q) and a confocal laser scanning microscope (model Zeiss, LSM 5 Pascal). A 40 $\times$  oil immersion objective with the appropriate filter sets for c-Fos (488 nm) and red retrobeads (543 nm) were used. Serial Z-stack images (1  $\mu$ m thick, 8–10 optical planes) through multiple sections were acquired (Axioplan 2 Imaging) using identical pinholes, gain and laser settings. c-Fos and retrobeads positive neurons were automatically counted using commercial software (Metamorph version 6.1; Molecular Devices, Sunnyvale, CA). c-Fos co-localization with retrobeads was manually quantified by an experimenter blind to experimental groups by measuring the percentage of retrogradely labelled neurons in both the PL and PVT expressing c-Fos.

**Virus-mediated gene expression.** The adeno-associated viruses (AAV, serotype 5) were obtained from the University of North Carolina Vector Core. Viral titres were  $3 \times 10^{12}$  particles per ml for AAV5:CaMKII::eYFP and  $4 \times 10^{12}$  particles per ml for AAV5:CaMKII $\alpha$ ::eNpHR3.0-eYFP. The use of CaMKII promoter enables transgene expression favouring pyramidal neurons<sup>22</sup>. Viruses were housed in an  $-80^\circ\text{C}$  freezer. Dual optical fibres (0.22 NA, 200  $\mu$ m core; 10 mm length, Doric Lenses, Quebec, Canada) were implanted in the PL, whereas single optical fibres were implanted singly in the PVT or bilaterally in the CeA and BLA (0.22 NA, 200  $\mu$ m core, 13 mm length, Doric Lenses).

**Illumination.** Yellow laser light was generated by a 593.5-nm diode-pumped solid-state laser (DPSS, MGLF 593.5; OEM Laser Systems). The beam was passed through a shutter/coupler (200  $\mu$ m core, Ozoptics), patchcord (200  $\mu$ m core, Doric Lenses), rotary joint (200  $\mu$ m core, 1  $\times$  2, Doric Lenses), mono or dual patchcord (0.22 NA, 200  $\mu$ m core, Doric Lenses), and optical fibre to reach the brain. The power density estimated at the tip of the optical fibre was 5 mW for illumination of somata and 10 mW for illumination of projection sites. The laser was initiated 10 s before tone onset, given the long response latencies observed in some PL and PVT neurons (see Extended Data Fig. 6), and persisted throughout the 30 s tone. Rats were familiarized with the patchcord for at least 3 d before starting each behavioural session.

**Optrode recording.** Rats infected with eNpHR-eYFP in the PL were anaesthetized with urethane (1 g kg<sup>-1</sup>, i.p.; Sigma-Aldrich) and placed in a stereotaxic frame. An optrode consisting of an optical fibre surrounded by 8 single-unit-recording wires (NB Labs) was inserted and directed towards the PVT ( $-3.1$  mm anterior, 1.8 mm lateral, 5.5 mm ventral from the bregma with a 20 $^\circ$  angle). The optrode was ventrally advanced in steps of 0.03 mm. Single units were monitored in real time (RASPUTIN software, Plexon Inc.). When a single unit was isolated, a 593.5 nm laser was activated for 10 s within a 20 s period, at least 5 times. Single units were recorded and stored for spike sorting (Offline Sorter, Plexon Inc.) and spike-train analysis (Neuroexplorer, NEX Technologies) as described below.

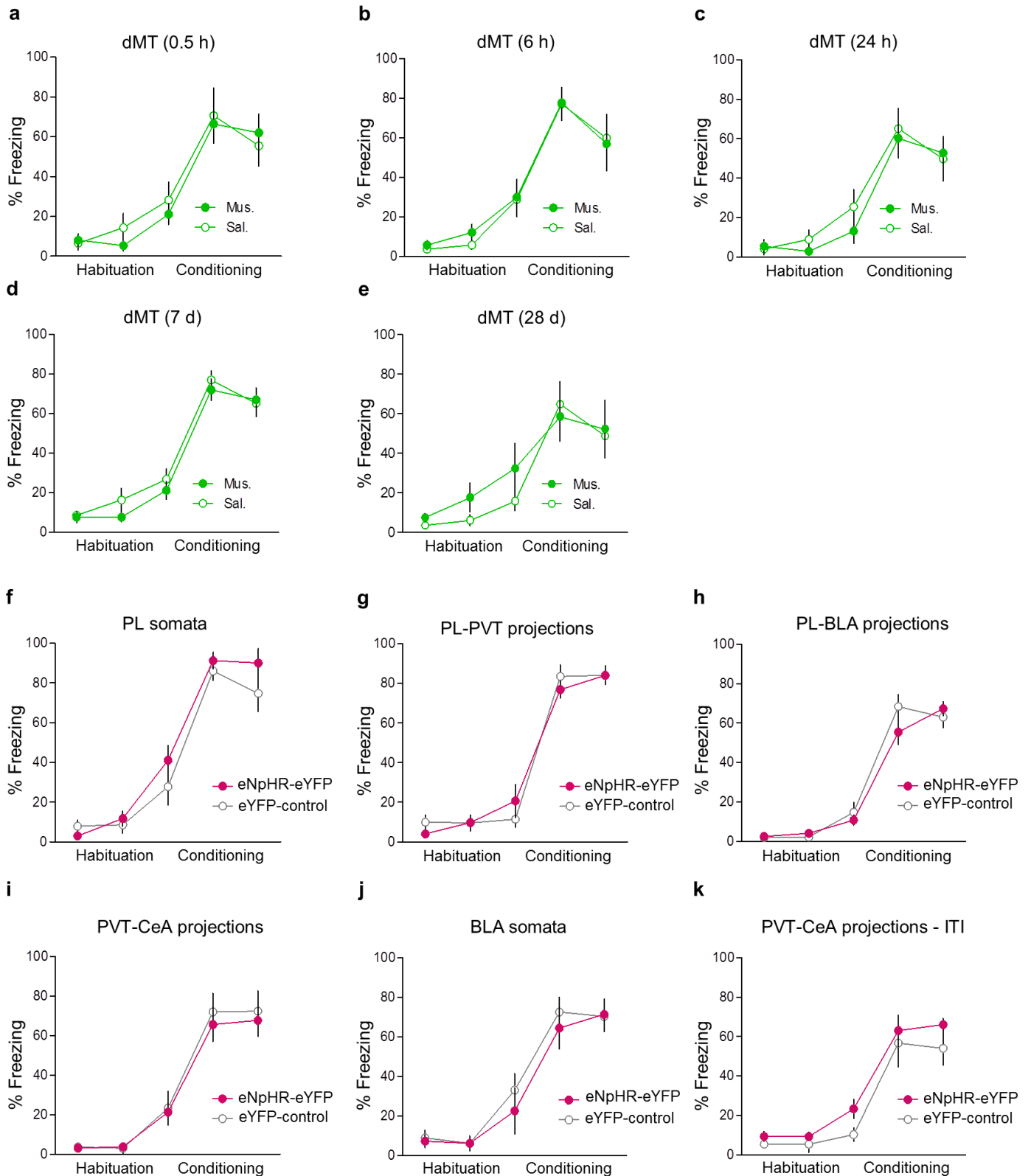
**Single-unit recording.** Rats were implanted with electrode arrays consisting of 16 fine wires (50  $\mu$ m, 2  $\times$  8, NB Labs). Stereotaxic coordinates for PVT electrodes were: AP,  $-1.8$  to  $-3.8$  mm; ML,  $\pm 1.8$  mm; and DV,  $-5.5$  mm, with a 20 $^\circ$  angle. Rats were fear conditioned and tested for fear retrieval with 4 tones presented at 2 h and 24 h after conditioning. Eleven rats were used, with 2–9 neurons per rat for a total of 54 neurons. Waveforms exceeding a voltage threshold were amplified (gain  $\times 100$ ), digitized at 40 kHz (MAP, Plexon) and stored onto disk. Single units were classified as maintained throughout all time points (pre-conditioning, 2 h, and 24 h) based on waveform features such as valley-to-peak and amplitude measurements

(Offline Sorter; Plexon; Extended Data Fig. 7)<sup>31</sup>. Automated processing was carried out using a valley-seeking scan algorithm and then evaluated using sort quality metrics. Spikes with interspike intervals  $< 1$  ms were excluded. Spike trains were analysed with commercial software (Neuroexplorer, NEX Technologies) for calculating firing rate and tone responses. Tone responses for 100-ms bins were calculated as  $z$  scores normalized to ten pre-tone bins of 100 ms. Significantly tone-responsive neurons showed  $z$  scores  $> 2.58$  ( $P < 0.01$ , two-tailed paired  $t$ -test) in either the first or second 100 ms bin following tone onset. Spontaneous firing rate was collected before the conditioning session and before both retrieval sessions for 3 min. Between recording sessions, rats were unplugged and returned to their home cage. At the end of the recording sessions, a micro-lesion was made by passing anodal current (0.25 mA for 25 s) through the active wires to deposit iron in the tissue. After perfusion, brains were extracted and stored in a 30% sucrose/ 6% ferrocyanide solution to stain the iron deposits.

**Data collection and analysis.** Behaviour was recorded with digital video cameras (Micro Video Products) and freezing was measured using commercially available software (Freezescan, Clever Systems). Press rate was measured using automated software (Graphic State, Coulbourn Instruments, Allentown, PA, USA). Distance travelled in the open field was measured using an automated video-tracking system (ANY-maze, Stoelting Co). Although experimenters were not blind to group allocation, automated counting was used for most measurements. Manual counting was only used to quantify the percentage of co-labelling between c-Fos and retrobeads (Fig. 3f,g) and was done by an experimenter blind to experimental groups. Parametric analysis was used since the data did not deviate substantially from a normal distribution (Shapiro–Wilk normality test,  $P > 0.05$ ). Similar variance was observed in all the groups statistically compared ( $F$ -test two-sample for variance before  $t$ -test, Bartlett's Chi-square test before ANOVA;  $P > 0.05$ ). All graphs and numerical values in the figures are presented as mean  $\pm$  s.e.m. Trials were averaged in blocks of two and compared with repeated-measures analysis of variance (ANOVA), followed by Tukey's post-hoc comparisons when appropriate (STATISTICA; Statsoft). All Student's  $t$ -tests used were two-tailed. A small percentage of rats (3%) were excluded from analysis because they did not exceed criteria for acquisition of conditioned freezing ( $> 30\%$  freezing in at least one trial). No further exclusions were made.

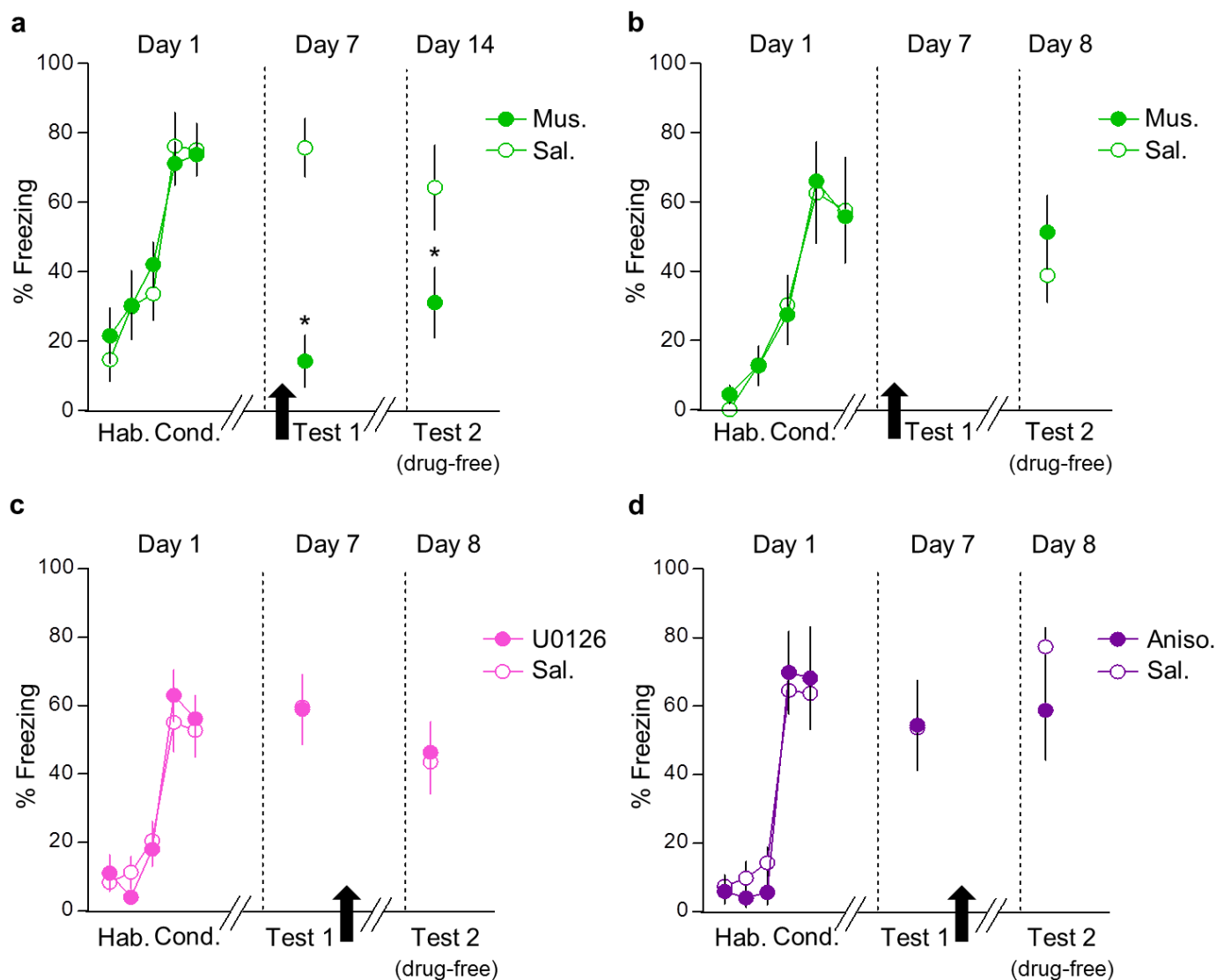
27. Quirk, G. J., Russo, G. K., Barron, J. L. & Lebron, K. The role of ventromedial prefrontal cortex in the recovery of extinguished fear. *J. Neurosci.* **20**, 6225–6231 (2000).
28. Paxinos, G. & Watson, C. *The Rat Brain in Stereotaxic Coordinates* 6th edn (Academic, 2007).
29. Schafe, G. E. *et al.* Activation of ERK/MAP kinase in the amygdala is required for memory consolidation of pavlovian fear conditioning. *J. Neurosci.* **20**, 8177–8187 (2000).
30. Nader, K., Schafe, G. E. & Le Doux, J. E. Fear memories require protein synthesis in the amygdala for reconsolidation after retrieval. *Nature* **406**, 722–726 (2000).
31. Tseng, W. T., Yen, C. T. & Tsai, M. L. A bundled microwire array for long-term chronic single-unit recording in deep brain regions of behaving rats. *J. Neurosci. Methods* **201**, 368–376 (2011).





**Extended Data Figure 1 | Conditioning levels in muscimol and optogenetic experiments.** **a–e**, In the muscimol experiments, levels of freezing to tones (pre-treatment) for the habituation phase (first two blocks) and conditioning phase (last three blocks) were similar for saline (Sal., white circles) and muscimol (Mus., green circles) groups at 0.5 h (**a**), 6 h (**b**), 24 h (**c**), 7 d (**d**) and 28 d (**e**). **f–k**, In the optogenetic experiments, freezing levels were similar for the

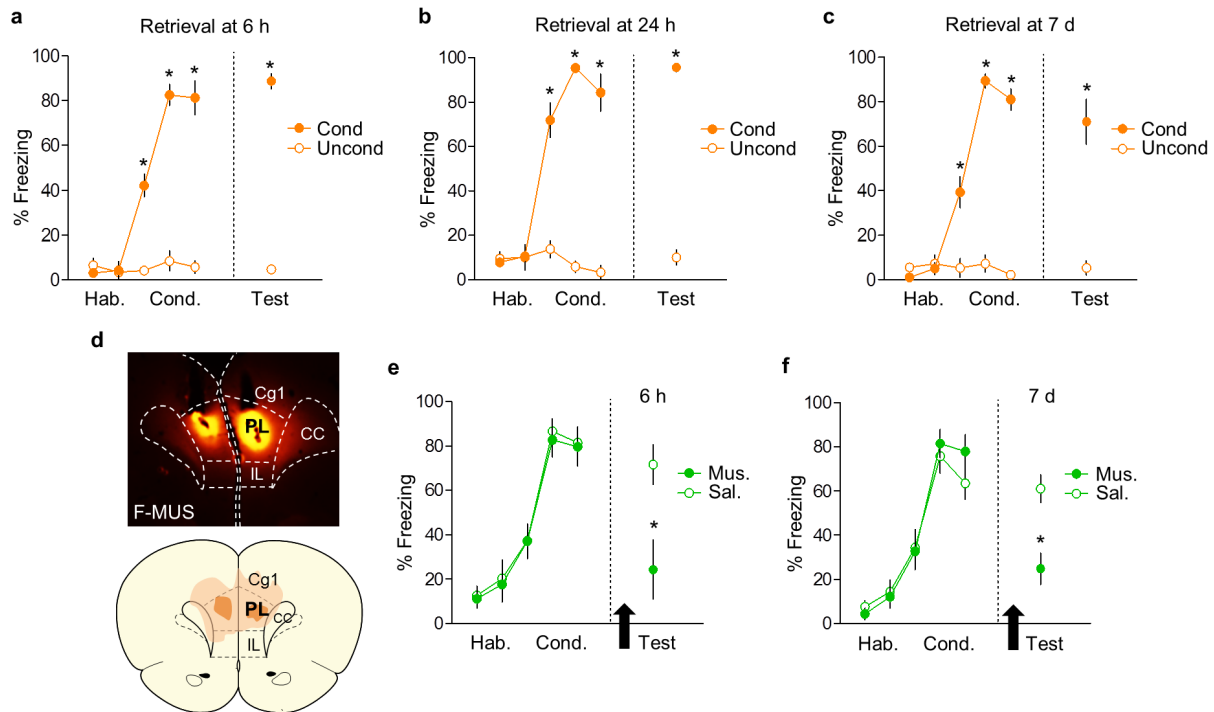
eNpHR-eYFP groups (red circles) and the control groups (white circles) before manipulation of the following regions or pathways: PL-somata (**f**); PL-PVT projections (**g**); PL-BLA projections (**h**); PVT-CeA projections (**i**); BLA somata (**j**); and PVT-CeA projections during inter-trial interval (ITI) (**k**). Data are shown as mean  $\pm$  s.e.m. in blocks of two trials.



**Extended Data Figure 2 | Neural activity in dMT, but not the MAPK cascade or protein synthesis in dMT, is necessary for memory maintenance following reactivation.** **a**, Freezing to tones during habituation (Hab.; first two blocks of day 1), conditioning (Cond.; last three blocks of day 1), test 1 (day 7), and test 2 (drug-free test; day 14) performed 7 days after dMT infusion of saline (Sal., white circles,  $n = 10$ ) or muscimol (Mus., green circles,  $n = 14$ ), in rats never given bar-press training. Infusion of Mus. into the dMT impaired fear retrieval during test 1 ( $t = -4.35$ ,  $P < 0.001$ ), and also 1 week later during test 2 ( $t = -2.14$ ,  $P = 0.04$ ). **b**, Freezing to tones during habituation (Hab.; first two blocks of day 1), conditioning (Cond.; last three blocks of day 1) and drug-free test (day 8) performed 24 h after dMT infusion of saline (Sal.,  $n = 5$ ) or muscimol (Mus.,  $n = 7$ ). Rats were infused in their home cage

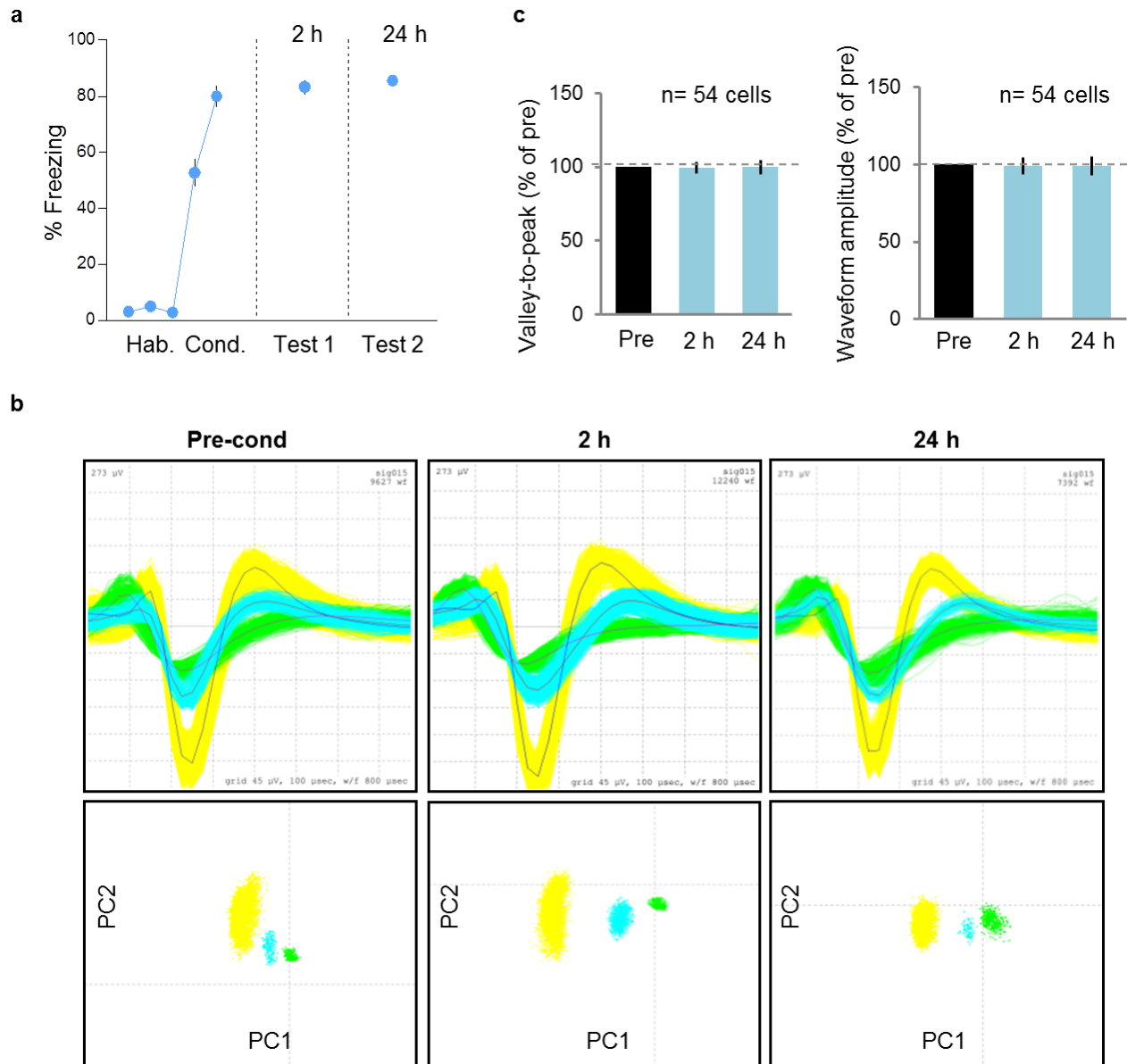
without fear reactivation. Mus. infused this way had no effect on fear retrieval the following day ( $t = -0.88$ ,  $P = 0.39$ ). **c**, Intra-dMT infusion of MAPK inhibitor U0126 ( $1 \mu\text{g}$  per  $0.5 \mu\text{l}$  per side,  $n = 11$ ) immediately after a two-tone test on day 7 did not alter freezing levels during a drug-free test performed the following day, compared to a vehicle control ( $n = 9$ ,  $t = 0.37$ ,  $P = 0.71$ ). **d**, Intra-dMT infusion of the protein synthesis inhibitor anisomycin (Aniso.,  $62.5 \mu\text{g}$  per  $0.5 \mu\text{l}$  per side,  $n = 7$ ) immediately after a two-tone test on day 7 did not alter freezing levels during a drug-free test performed the following day, compared to vehicle control ( $n = 5$ ,  $t = 1.33$ ,  $P = 0.21$ ). One-way repeated-measures ANOVA was used on day 1. Unpaired  $t$ -test between Sal. and Mus. groups were used on days 7, 8 and 14. Data are shown as mean  $\pm$  s.e.m. in blocks of two trials; \* $P < 0.05$ .





**Extended Data Figure 3 | Conditioning levels for c-Fos experiments, and the effects of PL inactivation at early versus late time points.** **a**, Freezing levels for conditioned ( $n = 4$ ) and un-shocked control ( $n = 5$ ) groups during fear conditioning and retrieval at the 6 h time point. The conditioned group showed a significant increase in freezing compared to controls ( $F_{(5,35)} = 76.12$ ,  $P < 0.001$ ). Hab., habituation; Cond., conditioning. **b**, Freezing levels for conditioned ( $n = 3$ ) and control ( $n = 4$ ) groups during fear conditioning and retrieval at the 24 h time point. The conditioned group showed a significant increase in freezing compared to controls ( $F_{(5,25)} = 40.07$ ,  $P < 0.001$ ). **c**, Freezing levels for conditioned ( $n = 5$ ) and control ( $n = 6$ ) groups during fear conditioning and retrieval at the 7 d time point. The conditioned group showed a significant increase in freezing compared to controls ( $F_{(5,45)} = 49.88$ ,

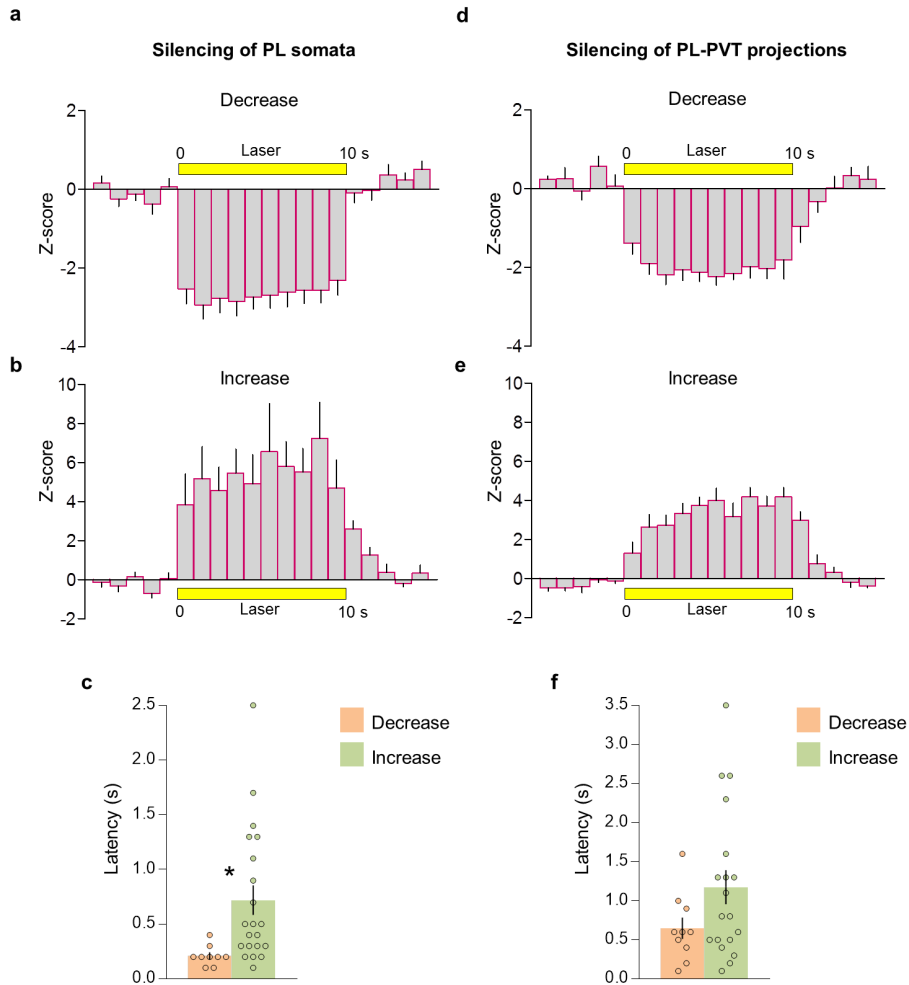
$P < 0.001$ ). Rats were perfused for c-Fos immunocytochemistry 90 min after the fear retrieval test. Repeated-measures ANOVA followed by Tukey's post-hoc test. **d**, Top, representative micrograph showing the site of fluorescent Mus. injection into the PL. Bottom, orange areas represent the minimum (darker colour) and the maximum (lighter colour) spread of muscimol into the PL. **e**, PL inactivation impaired fear retrieval at 6 h ( $F_{(1,11)} = 7.92$ ,  $P = 0.01$ ; Sal.,  $n = 6$ ; Mus.,  $n = 7$ ). **f**, In separate animals, PL inactivation also impaired fear retrieval at 7 d after conditioning ( $F_{(1,14)} = 13.8$ ,  $P = 0.002$ ; Sal.,  $n = 8$ ; Mus.,  $n = 8$ ). The retrieval test was performed 30 min after infusion of Sal. or Mus. (black arrows). One-way ANOVA followed by Tukey's post-hoc test. Data are shown as mean  $\pm$  s.e.m. in blocks of two trials; \* $P < 0.05$ .



**Extended Data Figure 4 | Conditioning levels for unit recording experiments, and waveform characteristics across recording sessions.**

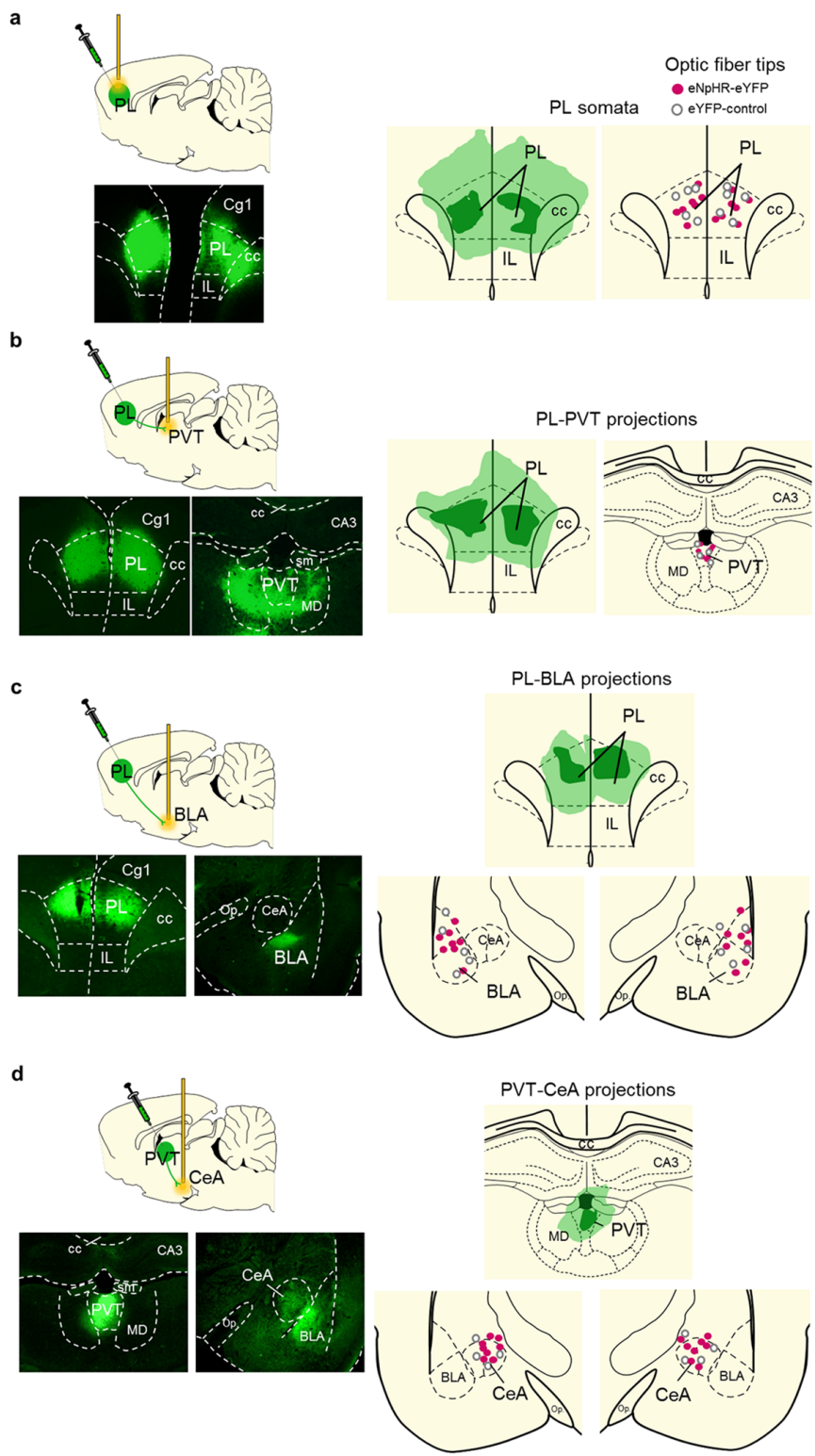
**a**, Freezing levels in response to tones during habituation (first two blocks), conditioning (last three blocks), test 1 (2 h) and test 2 (24 h) in rats never given bar-press training. Rats showed similar levels of freezing during retrieval at 2 h and 24 h after conditioning ( $n = 11$ ). Data are shown as mean  $\pm$  s.e.m. in blocks of two trials. **b**, Top, waveforms of three representative PVT neurons recorded during pre-conditioning (left), 2 h post-conditioning (middle), and

24 h post-conditioning (right). Bottom, principal component (PC) analysis of these cells' waveforms at all three time points. **c**, Average valley-to-peak time (left), and average waveform amplitude (right) for all neurons ( $n = 54$ ), shown as a percentage of pre-conditioning values. Of 54 neurons, 53 were unchanged (100% of pre-conditioning value) at both time points (2 h and 24 h) for one or both waveform parameters. One neuron showed 90% of pre-conditioning valley-to-peak time at both 2 h and 24 h, and ranged from 88 to 100% of pre-conditioning amplitude.



**Extended Data Figure 5 | Average firing rate and latency data for laser illumination of PL somata and PL terminals in the PVT expressing eNpHR-eYFP.** **a, b,** Average peri-stimulus time histogram of PL neurons that decreased (24 out of 50) (**a**) or increased (8 out of 50) (**b**) their firing rate during laser illumination of PL somata. **c,** Latency of PL neuronal responses to laser illumination of PL somata (paired Student's *t*-test,  $P = 0.02$ ). **d, e,** Average

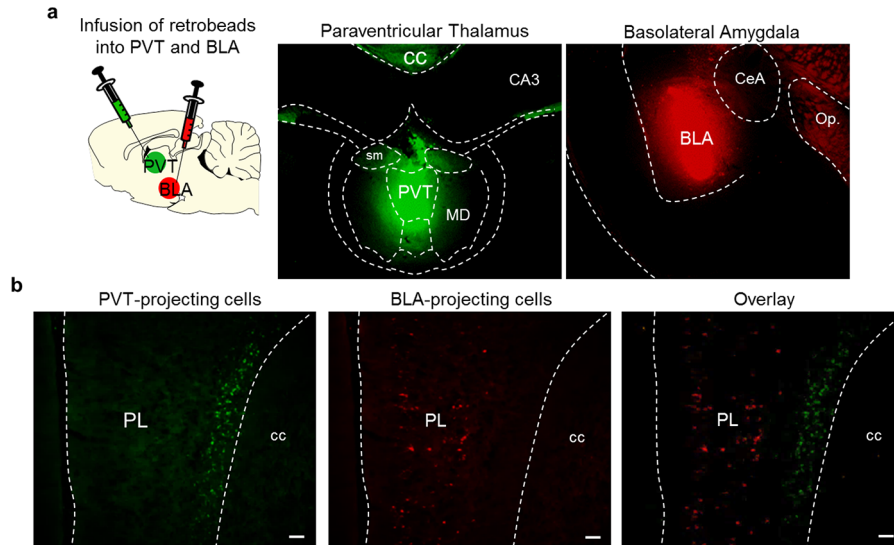
peri-stimulus time histogram of PVT neurons that decreased (13 out of 47) (**d**) or increased (9 out of 47) (**e**) their firing rate during laser illumination of PL terminals in the PVT. **f,** Latency of PVT neuronal responses to laser illumination of PL terminals in the PVT (paired Student's *t*-test,  $P = 0.11$ ). Peri-stimulus time histograms are shown in bins of 1 s. Response latency was measured in bins of 100 ms; \* $P < 0.05$ .



**Extended Data Figure 6 | Location of eNpHR-eYFP expression and optical fibres.** **a**, Left, representative micrograph showing eNpHR-eYFP expression in the PL. Right, placements of optical fibre tips in the PL. **b**, Left, representative micrograph showing the expression of eNpHR-eYFP in the PL and its terminals in dMT. Right, placement of optical fibre tips in the PVT. **c**, Left, representative micrograph showing the expression of eNpHR-eYFP in the PL

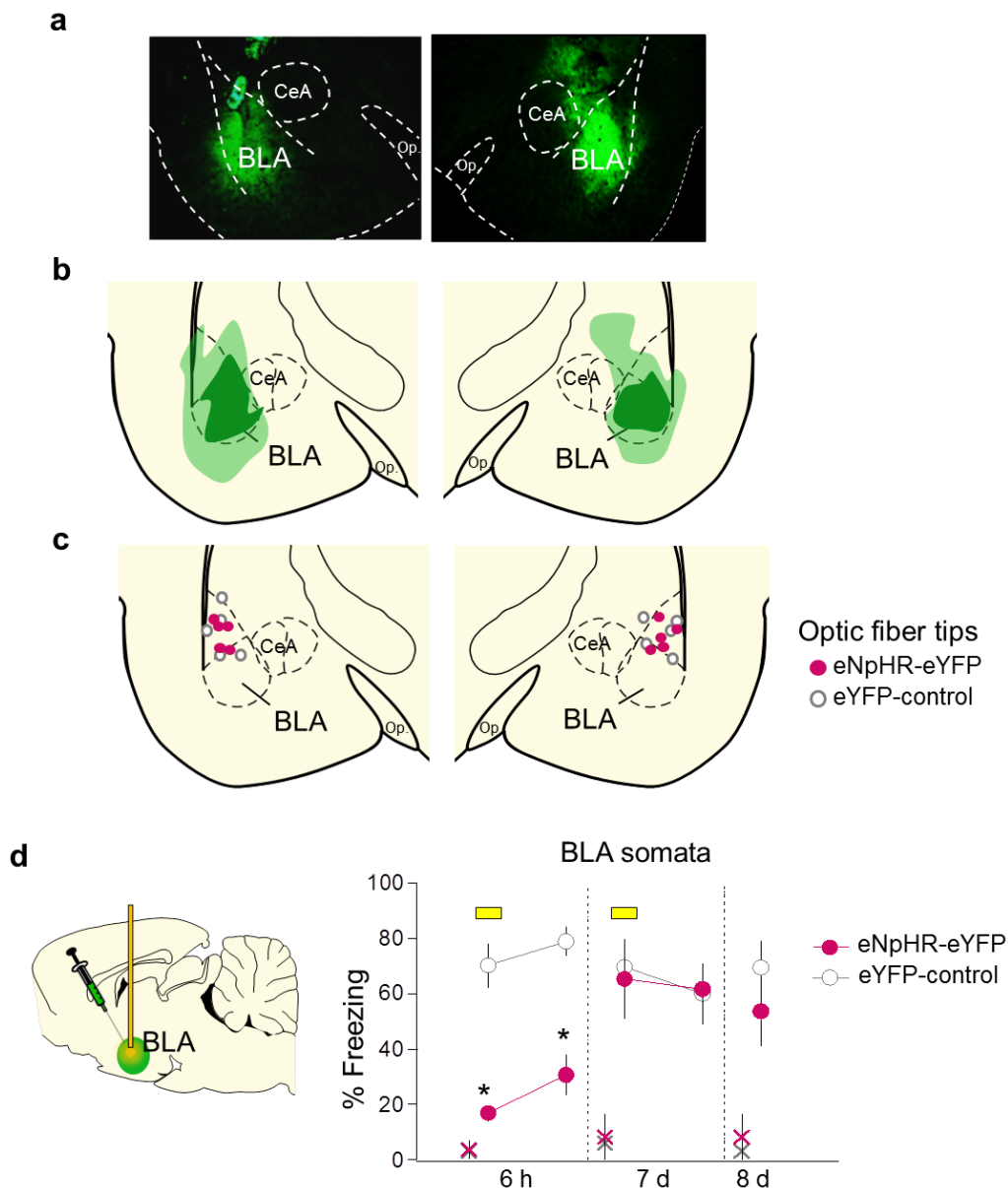
and its terminals in the amygdala. Right, placement of optical fibre tips in the BLA. **d**, Left, representative micrograph showing the expression of eNpHR-eYFP in the PVT and its terminals in the amygdala. Right, placement of optical fibre tips in the CeA. Micrographs were obtained 8–10 weeks after virus infusion. cc, corpus callosum; IL, infralimbic cortex; MD, mediodorsal thalamus; Op., optical tract; sm, stria medullaris.





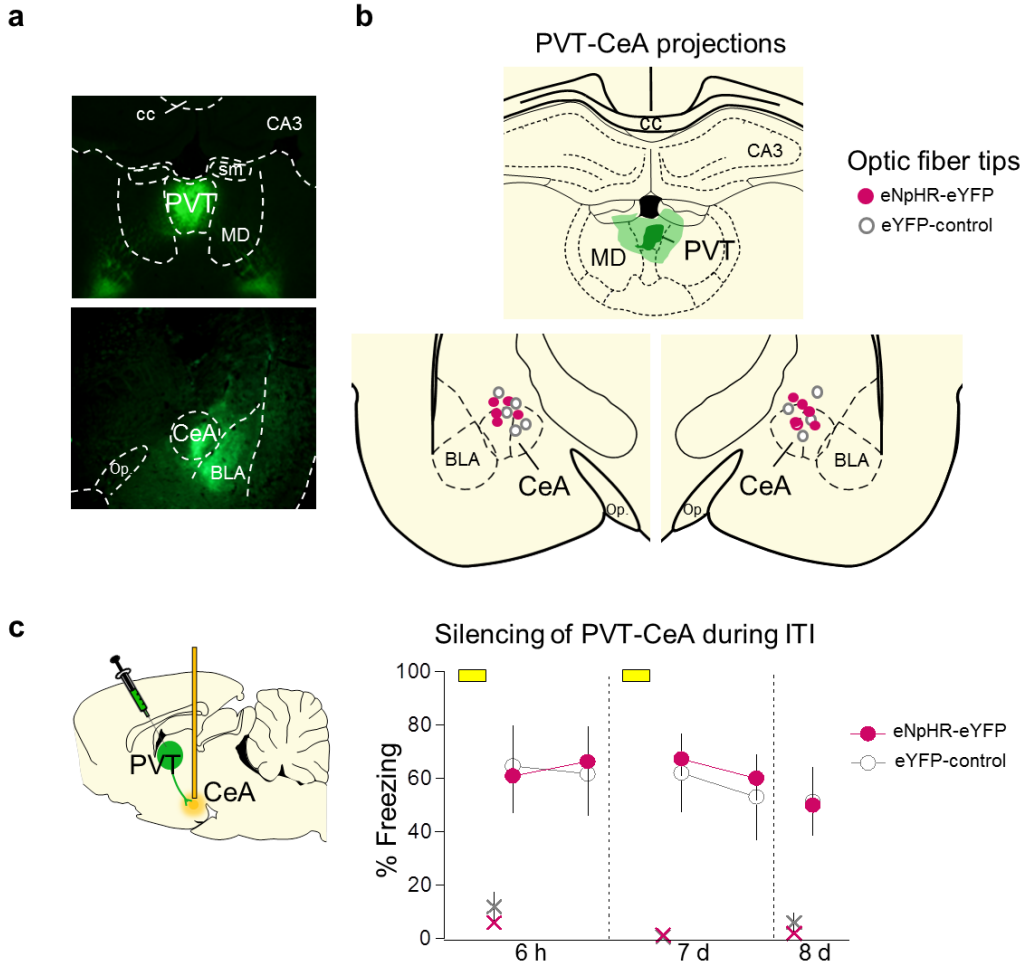
**Extended Data Figure 7 | PL neurons projecting to the PVT versus the BLA are located in distinct layers.** **a**, Left, schematic of retrobead injections. Middle, micrograph showing the site of retrobead infusion into the PVT (green), and right, micrograph showing the site of retrobead infusion into the BLA (red) in the same rat. **b**, Left, PL neurons retrogradely labelled from PVT

infusion (green). Middle, PL neurons retrogradely labelled from BLA infusion (red). Right, overlay image showing the absence of co-labelling between PL neurons projecting to the PVT (green, deep layers) and PL neurons projecting to the BLA (red, superficial layers). Scale bar, 100  $\mu$ m.



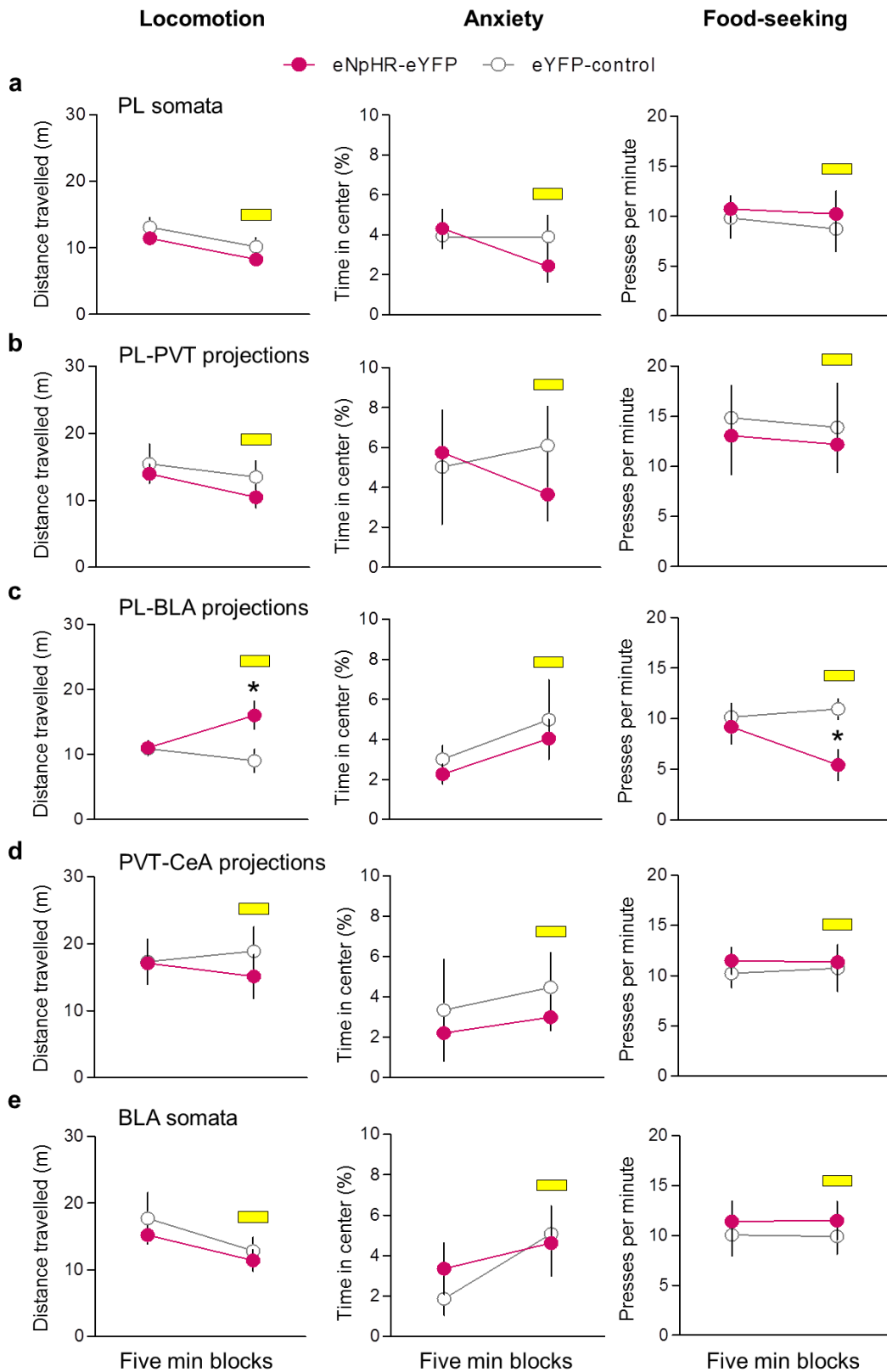
**Extended Data Figure 8 | Silencing BLA somata impaired fear retrieval at early, but not late, time points after conditioning.** **a**, Representative micrograph showing eNpHR-eYFP expression in the BLA. **b**, Green areas represent the minimum (darker colour) and the maximum (lighter colour) expression of eNpHR-eYFP in the BLA. **c**, Dots represent the location of optical fibre tips within the BLA. **d**, Illumination of BLA soma (yellow bar) reduced

freezing at 6 h ( $F_{(1,9)} = 54.6, P < 0.001$ ), but not at 7 d ( $F_{(1,9)} = 10.1, P = 0.91$ ) or 8 d ( $P = 0.33$ ), in the eNpHR-eYFP group ( $n = 5$ ) compared to eYFP control group ( $n = 6$ ). Repeated-measures ANOVA followed by Tukey's post-hoc test. Data are shown as mean  $\pm$  s.e.m. in blocks of 2 trials; \* $P < 0.05$ . 'x' symbols indicate baseline (pre-tone) freezing levels.



**Extended Data Figure 9 | Silencing PVT projections to the CeA during the inter-trial interval did not impair fear retrieval.** **a**, Representative micrograph showing the expression of eNpHR-eYFP in the PVT and its terminals in the amygdala. **b**, Top, green areas represent the minimum (darker colour) and the maximum (lighter colour) expression of eNpHR-eYFP in the PVT. Bottom, dots represent the location of optical fibre tips within the

CeA. **c**, Illumination (40 s) of PVT inputs to the CeA during the interval between tones (3 min) did not affect freezing at 6 h ( $F_{(1,8)} = 0.75, P = 0.40$ ), 7 d ( $F_{(1,8)} = 0.04, P = 0.84$ ), or 8 d ( $P = 0.93$ ), compared to the eYFP control group ( $n = 5$  per group). Repeated-measures ANOVA followed by Tukey's post-hoc test. Data are shown as mean  $\pm$  s.e.m. in blocks of 2 trials; \* $P < 0.05$ . 'x' symbols indicate baseline (pre-tone) freezing levels.



**Extended Data Figure 10 | Effects of laser illumination on locomotion, anxiety and food-seeking behaviour in rats expressing eNpHR-eYFP.**

**a–e,** Rats were tested in an open field during a 9 min session (3 min acclimation, 3 min laser off, 3 min laser on). We measured the total distance travelled (left) and the percentage of time spent in the centre of the apparatus (middle) to assess locomotor activity and anxiety, respectively. We also compared the rate of pressing for food (right) in a 15 min session (5 min acclimation, 5 min laser off, 5 min laser on). Silencing of PL somata (eNpHR-eYFP,  $n = 7$ ; control,

$n = 5$ ) (a), PL inputs to the PVT (eNpHR-eYFP,  $n = 5$ ; control,  $n = 5$ ) (b), PVT inputs to the CeA (eNpHR-eYFP,  $n = 7$ ; control,  $n = 5$ ) (d), or BLA somata (eNpHR-eYFP,  $n = 5$ ; control,  $n = 6$ ) (e) did not affect locomotion, anxiety or food-seeking. However, silencing PL-BLA projections (c) increased locomotion ( $F_{(1,12)} = 12.4, P = 0.004$ ; eNpHR-eYFP,  $n = 6$ ; control,  $n = 8$ ) and decreased food-seeking ( $F_{(1,15)} = 6.0, P = 0.02$ ; eNpHR-eYFP,  $n = 7$ ; control,  $n = 10$ ). Repeated-measures ANOVA followed by Tukey’s post-hoc test. Data are shown as mean  $\pm$  s.e.m.; \* $P < 0.05$ .